Reduction and Non-stoicheiometry of Niobium Pentoxide

By K. M. Nimmo and J. S. Anderson,* Inorganic Chemistry Laboratory, University of Oxford, Oxford OX1 3QR

The reduction equilibria and non-stoicheiometry of niobium pentoxide have been re-examined in order to correlate thermodynamic behaviour with structural modification during reaction. Equilibria were measured thermogravimetrically, by (T,x) scans in constant gas buffer mixtures, over oxygen activities 10^{-15}—10^{-19} atm at 900—1050 °C. Products of microbalance runs and of parallel preparations were characterized by electron diffraction and direct lattice imaging electron microscopy. The composition range traversed, $NbO_{2\cdot500}$ to $NbO_{2\cdot42}$, simulated the reversible bivariant behaviour of a non-stoicheiometric oxide, but structurally it was converted progressively from the H form of Nb_2O_5 to $Nb_{25}O_{62}$ to $Nb_{12}O_{29}$. These structures were generated in coherently intergrown lamellae and domains; the crystals do not behave as classical Gibbs phases, and the thermodynamic behaviour arises, in part, from gross hysteresis and ' hybrid crystal ' formation. The structures formed at 950—1050 °C are not in inner equilibrium, and at 1200—1300 °C rearrange to coherent intergrowth phases, $Nb_{53}O_{132}$ and $Nb_{39}O_{97}$. It is inferred that two distinct reaction processes are involved: an easy process that transforms one simple block structure into another, and a slow reshuffle of crystallographic shear planes to attain inner equilibrium. Some stoicheiometric variability of the structures is not excluded.

Niobium pentoxide is described as an extrinsic n-type semiconductor, becoming oxygen-deficient when it is equilibrated with a low chemical potential of oxygen at high temperatures. The behaviour has been investigated by a number of workers,[1-4] who have treated Nb_2O_5 as a classical non-stoicheiometric system, in which the quantitative relation between chemical potential of oxygen, composition, and conductivity could be expressed (1) in terms of point defect theory,

$$O^x \rightleftharpoons \tfrac{1}{2}O_2 + V_O^{\times};\ V_O^{\times} \rightleftharpoons V_O^{\cdot} + e^- \rightleftharpoons V_O^{\cdot\cdot} + 2e^- \quad (1)$$

through the creation of oxygen vacancies. The implication of the earlier work is that a non-stoicheiometric phase Nb_2O_{5-x} extends over a wide composition range, at least to $NbO_{2\cdot49}$,[5,6] and possibly down to a composition approaching $NbO_{2\cdot4}$.[3,4] Such a conclusion is in direct conflict with what is now known, especially from the crystallographic studies initiated by Wadsley and the chemical studies from Schäfer's school, about the existence of intermediate oxide phases in the composition range $NbO_{2\cdot0}$ to $NbO_{2\cdot5}$ and in the related ternary oxide systems. The supposed reduction equilibria should therefore be re-examined and related to the real structures traversed in the course of reduction and reoxidation reactions. We discuss here some results obtained in the range of temperatures and chemical potentials directly comparable with those used in the work on electronic conductivity and transport properties.

About 14 structurally distinct modifications of niobium pentoxide have been reported,[7] most of them thermodynamically metastable with respect to conversion into the high-temperature form H-Nb_2O_5 * (denoted α-Nb_2O_5 in the physical and older chemical papers). This form, with the unit-cell composition $Nb_{28}O_{70}$,[8] together with several other modifications (M-Nb_2O_5, N-Nb_2O_5, the new modification $Nb_{10}O_{25}$ recently obtained in this laboratory, and several others) is one of the group of complex oxides designated as ' block ' structures by Wadsley, Roth, and Andersson, as are the well defined mixed-valence oxides $Nb_{25}O_{62}$ ($NbO_{2\cdot480}$), $Nb_{22}O_{54}$ ($NbO_{2\cdot454}$), and $N_{12}O_{29}$ ($NbO_{2\cdot417}$)

* For the nomenclature of the several modifications of Nb_2O_5 see ref. 7.

[1] P. Kofstad and P. B. Anderson, *J. Phys. Chem. Solids*, 1961, **21**, 280.
[2] P. Kofstad, *J. Less Common Metals*, 1968, **14**, 153.
[3] R. N. Blumenthal, J. B. Moser, and D. H. Whitmore, *J. Amer. Ceram. Soc.*, 1965, **48**, 620.
[4] V. I. Lavrent'ev, Y. I. Gerasimov, and T. N. Rezukhina, *Proc. Acad. Sci. U.S.S.R.* (Phys. Chem), 1961, **136**, 201.
[5] R. Gruehn and H. Schäfer, *Naturwiss.*, 1963, **50**, 642.
[6] L. M. Kovba, V. K. Trunov, and Z. Y. Pol'shchikova, *Inorg. Materials*, 1967, **3**, 354.
[7] H. Schäfer, R. Gruehn, and F. Schulte, *Angew. Chem. (Internat. Edn.,)* 1966, **5**, 40.
[8] B. M. Gatehouse and A. D. Wadsley, *Acta Cryst.*, 1964, **17**, 545.

intermediate between Nb_2O_5 and NbO_2.[9] They are derived from the ReO_3 structural type, in which octahedral co-ordination groups (NbO_6) are linked by sharing their apical oxygen atoms. To achieve the requisite anion–cation site ratio, $Nb : O \leqslant 2 : 5$, edge sharing replaces apex sharing between co-ordination octahedra along certain crystallographic directions; the resulting sheets of edge-sharing octahedra, which have structures related to those of crystallographic shear planes in square tunnels that provide tetrahedral cation sites at $y = \frac{1}{4}, \frac{3}{4}$. Following the shorthand convention introduced by Allpress, the structures in Figure 1 are adequately represented by rectangles through the cation sites in the faces of each column.

This structural principle provides the most subtle flexibility in accommodating changes of stoicheiometry within partially or completely ordered structures. It is clear that the composition range spanned by the

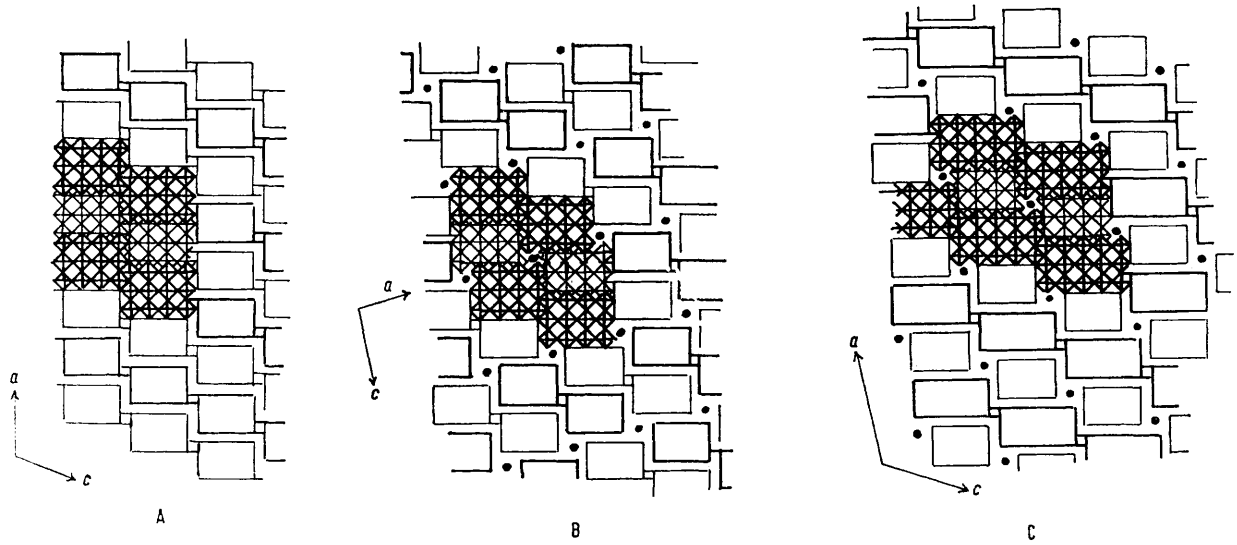

FIGURE 1 Structures of A, $Nb_{12}O_{29}$, $(4 \times 3)\infty$; B, $Nb_{25}O_{62}$, $(4 \times 3)_2$; C, H-Nb_2O_5, $Nb_{28}O_{70}$, $\{(5 \times 3)\infty + (4 \times 3)_1\}$, in [010] projection. Linkage of octahedra in columns and schematic representation

the Magneli phase oxides M_aO_{3a-b}, demarcate rectangular blocks or columns of ReO_3-type structure. These measure $(m \times n)$ octahedra in cross section and are infinite along the b axis of the crystal. The whole crystal is thereby built up from two sets of columns, with their cations at the levels $y = 0$ and $y = \frac{1}{2}b$ and, subject to the constraint that the assembly of interfaced columns should be space-filling, numerous combinations of column cross sections $(m \times n)$, $(m' \times n') \cdots$ can, in principle, generate either regular crystal structures, that should correspond to distinct compounds or crystal modifications, or defect structures, with a high degree of local order, involving not point defects, but columns of ' wrong ' cross section. In $Nb_{12}O_{29}$ (monoclinic form), columns 4×3 octahedra in section, at each level, are linked into infinite ribbons by further edge sharing between octahedra at the same level (Figure 1, A): the structure may be symbolized $(4 \times 3)\infty$. In $Nb_{25}O_{62}$ [Figure 1, B; symbol $(4 \times 3)_2$], 4×3 columns are paired at each level. In H-Nb_2O_5, $Nb_{28}O_{70}$, infinite ribbons of 5×3 columns at one level are combined with isolated 4×3 columns at the second level (Figure 1, C); the structure may be symbolized as $\{(5 \times 3)\infty + (4 \times 3)_1\}$. In $Nb_{25}O_{62}$ and $Nb_{28}O_{70}$ the junctions between the corners of columns define

[9] See A. D. Wadsley and S. Andersson, ' Perspectives in Structural Chemistry,' eds. J. D. Dunitz and J. A. Ibers, Academic Press, New York, vol. III, 1970.

reported non-stoicheiometry of niobium pentoxide, *i.e.*, by a bivariant equilibrium or pseudo-equilibrium in its dissociation, covers also the existence of at least three distinct structures, attributable to discrete compounds of definite, though complex, formula, which can apparently be converted into one another only by a complete reorganization of atomic positions and of the interfaces between blocks, throughout the crystals. These structures are derived from, and related dimensionally to, a common sub-cell: the ReO_3-type parent structure. Although the co-ordination octahedra are not perfectly regular and the interatomic distances (*e.g.* at the column interfaces and corner sites) vary slightly from one structure to another, they are almost perfectly compatible in dimensions; little error is introduced if they are described in terms of the common metric of an octahedral unit, 2·9 Å on each edge (*ca.* 4 Å diagonal). As has been pointed out,[10] this implies that perfectly coherent intergrowth is possible between one structure and another, across appropriate crystallographic planes. Thus the $Nb_{25}O_{62}$ structure can grow coherently with either the $Nb_{28}O_{70}$ structure (Figure 2, A) or the $Nb_{12}O_{29}$ structure (Figure 2, B). Such intergrowth could lead, in principle to extended contiguous domains of the two structures, to isolated

[10] (*a*) J. G. Allpress, J. V. Sanders, and A. D. Wadsley, *Acta Cryst.*, 1969, **25**, 1156; (*b*) J. G. Allpress and A. D. Wadsley, *J. Solid State Chem.*, 1969, **1**, 28; (*c*) J. G. Allpress, *ibid.*, p. 66.

strips of one structure within another (constituting an extended, 2-dimensional defect), or to regular alternation: a regular intergrowth structure, to be defined crystallographically as a discrete compound.

These considerations define a number of problems, for discussion in the light of the experimental evidence presented below: (*a*) the true equilibrium structures in the composition range; (*b*) the structural adaptation actually followed under the reaction conditions employed; (*c*) the role of kinetics in differences between actual and idealized behaviour; (*d*) the mechanism of reduction and oxidation processes; (*e*) the part played by point defects and extended defects in the structure and reactivity of the system.

A. *Equilibria in the* $NbO_{2\cdot5-x}$–O_2 *System.*—The free-energy surface in (μ,T,x) space (x = composition variable) must be mapped in sufficient detail to detect the formation of intermediate phases in a complex system, and to determine the composition ranges of monophasic solids. Of the methods that have been used for this and other systems, both solid-state galvanic cell measurements and gas equilibration methods have usually been used to provide $(\mu,T)_x$ or $(\mu,x)_T$ sections. In general, the density of data has been rather low, so that much information about the phase relations can be missed. Where it is applicable, *e.g.*, for systems with oxygen dissociation pressures in the range 10^{-3} atm $< p <$ 1 atm, continuous scans across $(T,x)_p$ sections provide the maximum sensitivity to fine structure in the free-energy surface;[11] they have the added advantage of enabling phase reactions to be initiated and completed with a minimum over- or under-saturation, a matter of importance when dissociation takes place in closely spaced successive stages, separated by small steps in μ_{O_2}. Chemical potentials in the niobium oxide system are, however, so low that they are attainable only by using gas buffer mixtures, *e.g.*, CO–CO_2. If the input buffer ratio (P_{CO}/P_{CO_2}) is denoted by r, in terms of the partial pressures of the mixture supplied to a flow system, a series of appropriately spaced temperature–composition scans, at constant input buffer ratios, provides a series of $(T,x)_r$ sections which have many of the advantages referred to. A thermogravimetric method was therefore adopted, in which the composition of a sample was followed as a function of temperature, in equilibrium with a constant feed of CO–CO_2 mixture.

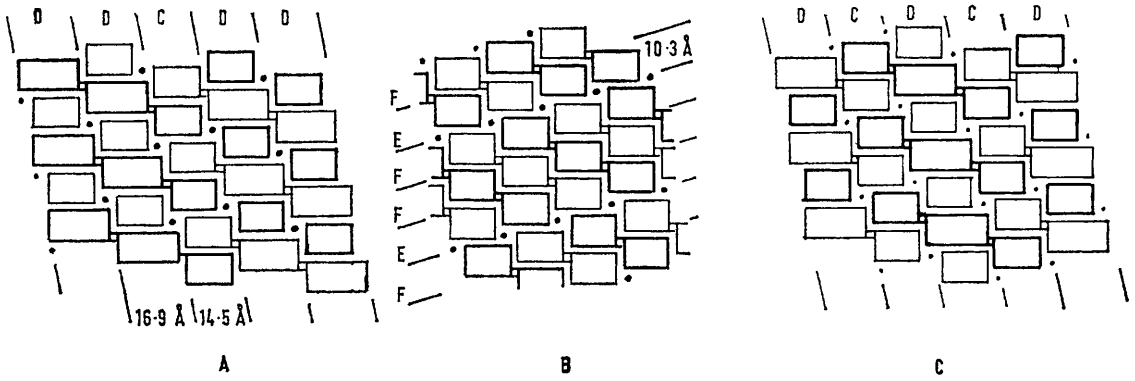

FIGURE 2 A, Coherent intergrowth of one row of $Nb_{25}O_{62}$ in H-Nb_2O_5 structure; B, Coherent intergrowth of one row of $Nb_{12}O_{29}$ in $Nb_{25}O_{62}$; C, Regular coherent intergrowth: C–D–C–D– · · · stacking in $Nb_{53}O_{132}$

EXPERIMENTAL

Niobium pentoxide was Johnson-Matthey Spec-Pure material. To ensure that it was used as the H-modification, and to improve its crystallinity for subsequent electron microscopy and diffraction, it was annealed at 1200—1400 °C in air before use.

Buffer gas mixtures were made up by two methods from compressed gases. Carbon monoxide (Air Products) had maximum levels of significant impurities stated to be not more than 750 p.p.m. oxygen and 1000 p.m. carbon dioxide. Whilst the latter could be removed, the former becomes important in making up high CO : CO_2 ratios, and must be allowed for. Carbon dioxide (Distillers) had water as principal impurity, with <10 p.p.m. carbon monoxide.

Kubaschewski, Evans, and Alcock [12] estimate the free energy of the reaction $4NbO_2 + O_2 \longrightarrow 2Nb_2O_5$ at 1223 K as −108,800 cal (mol O_2)$^{-1}$; combination with data for the CO–CO_2 equilibrium indicates that reduction would be complete for a CO : CO_2 ratio (r) 150—200. It can be estimated that ratios in the range $1 \leqslant r < 150$ would cover the composition range of interest at 1100—1320 K. For mixtures with $r \leqslant 15$, the gases were continuously delivered through calibrated Rotameter flow meters into the gas line. Suitable adjustment of the control valves gave constant flow rates over prolonged experiments; the total flow of buffer gas did not, in general, exceed 75 ml min^{-1}. The CO was passed through a tower of Linde molecular sieve 4A at room temperature to remove CO_2, but the oxygen impurity could not conveniently be removed. The CO_2 was freed from water by passage through molecular sieve 5A. Purification towers were wound with a heater, to enable them to be periodically regenerated *in vacuo* at 300 °C. After purification, the

[11] B. G. Hyde, D. J. M. Bevan, and L. Eyring, *Phil. Trans.*, 1966, *A*, **259**, 583.

[12] O. Kubaschewski, E. L. Evans, and C. B. Alcock, 'Metallurgical Thermochemistry,' 4th edn., Pergamon Press, Oxford, 1967.

gas streams were mixed and passed at 1 atm total pressure to a needle valve. Mixtures with $r > 15$, at the flow rates employed, are not readily obtained and controlled with sufficient precision by simple flowmeter methods. For these, a constant flow of CO was established. CO_2 was contained over CO_2-saturated, air-free water in a thermostatted reservoir, from which it was displaced by progressive, steady injection of water by means of a variable speed peristaltic pump. The CO_2 was introduced into the CO stream through a fine jet dipping under Apiezon oil. Since the CO_2, the minor constituent, contained water vapour at its room temperature saturation pressure, the mixed gases were dried by passage through a tower of Anhydrone before passing to the needle valve.

This needle valve joined the gas line to a Cahn RG electrobalance in a standard vacuum bottle. Gases passed through the balance *via* a second needle valve to the vacuum pump. The needle valve settings were adjusted so as to maintain a steady, measured pressure of 5 cmHg in the balance section. The balance chamber was screened from room-temperature fluctuations, radiation, and convection of air above the furnace and air was circulated across it by a fan. The specimen was contained in a platinum bucket (10 mm diam.), suspended from the balance arm by a 0·005 in diam. platinum wire, within a 20 mm i.d. silica tube. This was wound externally with Kanthal wire, and earthed, to eliminate troublesome electrostatic charging effects and electromagnetic noise. The weight of sample taken (*ca.* 100 mg) was chosen to give a weight change, during reduction or oxidation, that could be accommodated within the optimum setting of the balance control (mass dial 5·000). The output of the balance was fed to one pen of a two-pen Rikadenki recorder; suitable attenuation gave full-scale deflection for 100 μg weight change, equivalent to about 0·008 in x for 100 mg load of an oxide NbO_x. The recorder was modified by incorporating microswitches to be operated by the pen carrier at either end of its travel; these actuated a reversible motor, driving the helipot on the Cahn balance control box and restoring the pen to the other side of the chart. Changes of weight of any amount, within the selected sensitivity range, would thereby be recorded in either direction.

All the parameters of the experiments (load and sensitivity, dimensions of furnace tube, bucket, and suspension, operating pressure, gas flow speed, *etc.*) were selected to minimize instabilities, and the reproducibility and long-term stability were checked by suitable calibrations. Steady-state gas circulation in the furnace tube gave a small, apparent weight loss which was a reproducible, linear function of temperature. Apparent weight changes were also reproducible functions of gas flow rate. These effects could therefore be corrected in the evaluation of measurements. As operated, the balance trace showed a noise level not exceeding 2·5 μg peak-to-peak over long periods in a static atmosphere. With flowing gas, the noise level was not greatly increased. A conservative estimate of the overall precision, including noise level and corrections, is that the measurements are good to ±5 μg on 100 mg load (*i.e.*, to ±0·0004 in x for NbO_x).

The sample was heated by a furnace with two windings; the inner winding was the main power supply and the outer winding was energized to maintain constant temperature, within narrow limits, in response to a thermocouple in the uniform temperature zone, adjacent to the silica sample tube. The furnace temperature could be programmed to give uniform heating or cooling rates between 5 and 100 K h^{-1}, by backing off the thermocouple e.m.f. with the output from a helipot, driven at constant speed by a $\frac{1}{3}$ rev. h^{-1} motor and used to divide a selected fraction of the voltage from a mercury cell. Alternatively, the temperature control provided for stepwise phase reactions to proceed at constant temperature. As long as the sample weight remained constant or changed only within the 100 μg traverse of the recorder chart, the temperature followed the set heating programme. With the onset of a dissociation step, the recorder pen actuated a microswitch at the end of its first traverse of the chart; this disengaged the back-off voltage drive, and a constant temperature was maintained until the programmer was reset manually. Sample temperatures were measured by a Pt/Pt-30% Rh thermocouple inside the silica tube and close to the bucket; the signal from this thermocouple was fed to the second pen of the recorder.

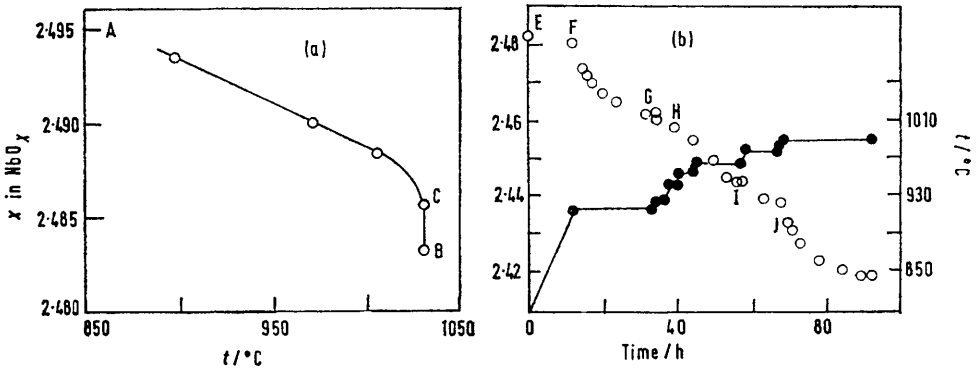

FIGURE 3 (a) Thermogravimetric temperature–composition curve in 15 : 1 CO–CO_2; (b) Composition–time (open circles) and temperature–time curves (full circles) in 30 : 1 CO–CO_2

RESULTS

At the oxygen potentials used in these experiments, slow loss of oxygen can be detected above *ca.* 650 °C. Above 850 °C, the weight loss responded sensitively and immediately to changes of temperature (usually 10 K h^{-1}), and weight was regained reversibly if the temperature programme was reversed. For the gas buffers of highest CO_2 content ($r = 10$, 15), the sample came to a composition around $NbO_{2.495}$ at the starting temperature for

each scan. The range $NbO_{2.5000}$ to $NbO_{2.495}$ was therefore not accessible in these measurements.

Characteristic features of the equilibration process, relevant to the discussion of all the evidence, can be seen from Figure 3. At relatively high oxygen potentials [Figure 3(a), $r = 15$], the composition of the oxide accommodated smoothly to change of temperature, from the initial value $NbO_{2.495}$ at A down to about $NbO_{2.487}$; the

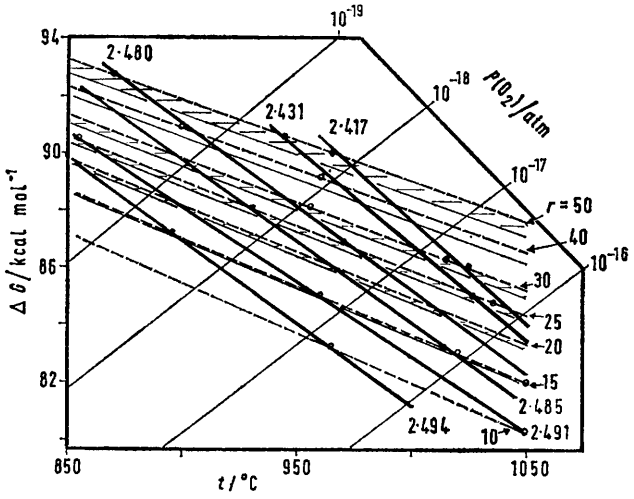

FIGURE 4 Ellingham plot of pseudo-equilibrium oxygen potentials for six (arbitrary) compositions from thermogravimetric experiments

dissociation reaction then accelerated. At C the temtemperature was held constant; oxygen loss continued isothermally down to $NbO_{2.483}$, at which point (B), further drift of composition became exceedingly slow. At 1050 °C in this buffer, the sample attained a final composition $NbO_{2.480}$. On this evidence, the segment AC could be interpreted as reflecting a bivariant equilibrium, with a non-stoicheiometric $NbO_{2.5-x}$ solid phase, and the segment CB a phase reaction with the limiting $NbO_{2.5-x}$ and a phase $NbO_{2.480+y}$ coexisting. Microbalance runs at lower oxygen potentials [Figure 3(b); $r = 30$] showed that this interpretation is too simple. There was again a steady weight loss EF, with an acceleration of the reaction at about $NbO_{2.480}$, but no stepped curve corresponding to a univariant equilibrium. Under isothermal, isobaric conditions FG the rate of weight loss slowed down; the composition approached a steady value but continued to drift slowly. A small increase in temperature produced immediate acceleration of the reaction (G, H, I, J); wherever the temperature was held steady, reaction decelerated and composition approached a final limit. Finally, above 1025 °C, the composition attained a final value very close to $NbO_{2.42}$; there are good grounds for accepting a univariant equilibrium [a step in the $(T,x)_r$ scan] between the phase $Nb_{12}O_{29}$ (ideal composition $NbO_{2.417}$) and NbO_2.

It is clear that an interpretation in terms of successive bivariant and univariant equilibria would be oversimplified; the observations resemble rather the behaviour of a system with gross hysteresis. Nevertheless, measurements made in separate experiments, traversing different sections of (T,x,r) space are mutually consistent. Figure 4 shows what is essentially an Ellingham diagram of $\bar{G}_{O_2}$ against T for the gas buffer mixtures used. To allow for the uncertainty in the residual oxygen (and CO_2) content of the carbon monoxide, together with the error limits for the free energy of oxidation of CO to CO_2, the calculated line for each buffer mixture is broadened into a band which brackets the maximum uncertainty. On these bands are superposed the observed 'equilibrium' data for a series of constant compositions NbO_x; since the thermogravimetric scans reveal no singularities or univariant steps, these compositions have been arbitrarily chosen and (except for the end product of controlled reduction $NbO_{2.417}$) have no special significance. For each of the compositions, the experimental points fall fairly well on a linear plot. The line for $NbO_{2.417}$ almost certainly approximates fairly well to that for the thermodynamically defined reaction (2). From the evidence of the thermogravimetric runs,

$$\tfrac{2}{5}Nb_{12}O_{29} \rightleftharpoons \tfrac{24}{5}NbO_2 + O_2 \qquad (2)$$

and from the structural considerations discussed below, none of the lines corresponding to other compositions can be ascribed to a thermodynamically defined process, even though the measurements simulate a non-stoicheiometric system in which $\bar{S}_{O_2}$ is roughly constant and $\bar{H}_{O_2}$ a function of composition. It would, therefore, not be justifiable either to extract thermodynamic data from the results or to compare them with any equilibrium defect model. Phenomenologically, and for comparison with the results of others, it is convenient to summarize the self-consistent behaviour by the (T,x) isobars of Figure 5.

Several earlier studies of Nb_2O_5 have been carried out in the same range of temperatures and oxygen potentials as is considered here. Those relating to semiconducting properties have been largely concerned with apparently truly reversible equilibria at higher oxygen potentials (*i.e.*, with $NbO_{2.5-x}$; $x \ll 0.005$) for which H-Nb_2O_5 may, perhaps, be an uncomplicated non-stoicheiometric compound. Treatment of the results in terms of point defect

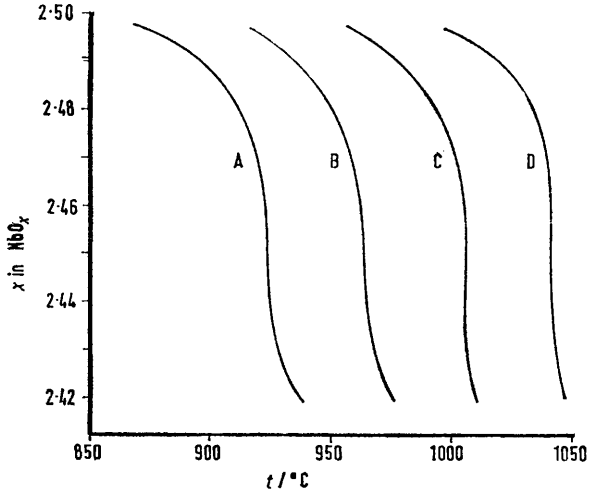

FIGURE 5 Temperature–composition isobars (smoothed) from thermogravimetric experiments. Oxygen pressure A, 10^{-19}; B, 10^{-18}; C, 10^{-17}; and D, 10^{-16} atm

formation and ionization equilibria may therefore be permissible, but absolute carrier concentrations were not derived and results can be compared with direct measurements of equilibrium composition only indirectly, through the pressure-dependence of the conductivity. Direct thermogravimetric measurements of the equilibrium have been made by Kofstad and Anderson [1] (900—1400 °C,

10^{-7} atm > P_{O_2} > 10^{-18} atm), who used much too short equilibration times, and by Blumenthal, Moser, and Whitmore [3] (900—1200 °C, 10^{-10} atm > P_{O_2} > 10^{-19} atm), who also measured oxygen potentials by a solid-state galvanic cell method. Close to stoicheiometry (for oxide less reduced than about $NbO_{2.495}$ at 900 °C or $NbO_{2.490}$ at 1200 °C) the somewhat scattered results seem compatible with the P^{-6} dependence upon oxygen pressure expected for the formation of doubly ionized point-defect oxygen vacancies; Kofstad and Anderson, indeed, considered that this model was valid down to much lower oxygen contents. The more extensive measurements of Blumenthal *et al.* show a good deal of scatter, but approximate to the same kind of smooth relationship as has been found here, for compositions traversing several distinct structural fields. In Figure 6 these older results and our own are

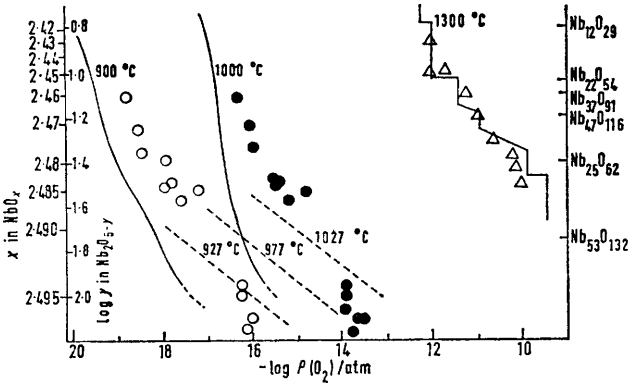

FIGURE 6 Isotherms of equilibrium oxygen pressure as a function of composition (plotted as log y in Nb_2O_{5-y}). Solid lines: this work. Broken lines: Kofstad and Anderson, ref. 1. Circles: Blumenthal *et al.*, ref. 3 at ○, 900 °C; and ●, 1000 °C. 1300 °C isotherm: Schafer *et al.*, ref. 13. △ Abbatista *et al.* 1250 °C isotherm, ref. 14. Note that steps on the 1300 °C isotherm do not coincide with the ideal formulae of $Nb_{53}O_{132}$, $Nb_{25}O_{62}$, and $Nb_{47}O_{116}$

compared, in the form of (p,x) isotherms, by use of a composition scale which, as must be emphasized, represents the effective [Nb^{4+}] but bears no necessary relation to the concentration of lattice defect.

Two (p,x) isotherms have been determined at higher temperatures. These differ significantly from the behaviour observed at 1100 °C or below. Schäfer, Bergner, and Gruehn [13] equilibrated Nb_2O_5 with a series of H_2–H_2O buffer mixtures at 1300 °C. They found that equilibrium was reached only slowly and, although the density of data is low, they clearly established that the 1300 °C isotherm has a succession of discrete phases, with narrow ranges of homogeneity, separated by univariant, phase-coexistence steps. Further, the discrete phases could be correlated with the intermediate oxides known from crystallographic work. A high-temperature isotherm (1250 °C), obtained by progressive reduction with CO–CO_2 mixture, has also been reported by Abbatista *et al.*[14] This (also shown in Figure 6) is stepped, giving an indication that intermediate phases are formed, but their attributed compositions bear little relation to the known structures in the system, and from the scanty description of the experimental method employed it appears that only qualitative significance can be attached to the work.

[13] H. Schäfer, D. Bergner, and R. Gruehn, *Z. anorg. Chem.*, 1969, **365**, 31.

In summary, it has been established that a pseudo-equilibrium response of oxide composition to oxygen potential simulates bivariant behaviour over the complete composition range from $NbO_{2.500}$ to $NbO_{2.42}$. This is consistently reproducible, and is reversible, at least for small excursions from equilibrium. A very slow drift of the compositions attained indicates that it is not a true equilibrium. The results of Schäfer *et al.* prove that, at temperatures where solid-state diffusion is operative, although slow, the pseudo-bivariant equilibrium breaks up into a succession of univariant equilibria. Further understanding requires a knowledge of the real structure of the solid phase in the pseudo-bivariant range.

B. *The Structure of Partially Reduced Niobium Pentoxide.*—The structures of these materials make phase analysis by X-ray methods difficult. Standard Debye–Scherrer methods are useless. The structures are related and the smaller interplanar spacings are dominated by the ReO_3-type sub-cell; the true cells are large and their diffraction patterns complex and similar. High-resolution Guinier methods have been used extensively by Schäfer and others to characterize the phases; structures of individual intermediate oxides (and the isostructural ternary oxides, such as $TiNb_{24}O_{62}$ and $Ti_2Nb_{10}O_{29}$) have been established by single-crystal work. Analysis of mixtures of phases, and especially the detection and identification of minor components, can be inconclusive in these circumstances. In particular, if (as proves to be the case) new structures are created in very small domains, the intensity of new contributions to the complex diffraction pattern can be reduced to background level by the resultant line broadening. Although it has been shown that a single crystal of H-Nb_2O_5 may retain its integrity throughout the reduction and reoxidation processes, true equilibration of crystals large enough for single-crystal X-ray work is difficult, and much real information, as distinct from statistics of site occupancy, may be lost. The most suitable techniques for structural investigation are selected-area electron diffraction, giving single-crystal data from sub-micron areas of crystal, together with direct lattice imaging methods to reveal structural singularities at the dimensional level of the unit cell.

EXPERIMENTAL

Most of the work reported was carried out on a JEM 6A electron microscope equipped with a goniometer stage, with 100 kV electrons. Some critically important results were obtained with a JEM 100U instrument by courtesy of JEOL (U.K.) Ltd. Specimens were prepared for microscopy by grinding under pentyl acetate and collecting fine fragments on carbon-coated copper grids. Structures in this series of compounds can be identified, and disorder detected, only in ($h0l$) reciprocal lattice sections; with their common b axis, one octahedron in depth, and long a and c axes, the (hkl) reciprocal lattice sections are not informative. Only a small proportion of crystal fragments on any grid lie so that they can be oriented with [010] parallel to the electron beam; of these, only a minority have extensive

[14] F. Abbatista, G. Chiantaretto, and E. V. Tkachenko, *Atti Acad. Sci. Torino*, 1968, **102**, 866.

areas or edges thin enough for lattice imaging. Hence the statistics of examination are unavoidably poor, although there is no evidence of any selective effects.

Diffraction patterns of the principal phases were identified from (*h*0*l*) projections and indexed by use of the crystallographic data. One-dimensional lattice fringe imaging methods were used in this work, by tilting the crystals from the symmetrical [010] orientation so that the desired reciprocal lattice row [*e.g.*, the (*h*00) or (00*l*) row] lay tangent to the Ewald sphere; a 60 μm aperture was used to select the central beam and adjacent beams for bright field fringing. In general, a through-focus series was photographed.

Under these conditions, a perfect crystal generates a set of uniformly spaced fringes, at a spacing corresponding to the interplanar spacing between the crystallographic planes selected [*e.g.*, 16·9 Å for (001) fringes from H-Nb_2O_5]. Interpolation of a lamella of different structure, with a different spacing, one or more unit cells in thickness gives a corresponding local anomaly in the fringe spacings, which were measured by microphotometry of the plates. By fringe imaging in two directions [*e.g.*, with the (100) and (001) lattice fringes of the host structure] the dimensional characteristics of any singularity could be identified and an unambiguous structure could usually be assigned to it in terms of the crystal chemical principles underlying the ' block ' structures. It was not necessary, for this purpose, to make specific assumptions about the correlation of contrast maxima and minima with structural details.

Standard techniques of bright-field and dark-field microscopy, at lower resolution, gave evidence of coherent domain intergrowth of one structure with another, observable in diffraction contrast. Further textural evidence was furnished by streaking in diffraction patterns. For any narrow element of structure, reciprocal lattice points are elongated into spikes, normal to the bounding surfaces. For narrow domains bounded by (*h*0*l*) planes, these spikes will lie in the reciprocal lattice projection employed, giving correspondingly streaked spots along the *h*0*l* direction concerned.

RESULTS

Electron microscopy showed that the initial Specpure Nb_2O_5, annealed at 1200—1450 °C, formed highly perfect crystals, occasionally containing lamellae or larger areas twinned on (10$\bar{1}$). This is the normal twinning habit, and we discuss the structure of the twin interface elsewhere. Material reoxidized to Nb_2O_5 after a microbalance run showed considerable disorder within the crystals, many of which had a diffraction pattern, heavily streaked along 10$\bar{1}$, indicative of narrow slabs of homogeneous structure bounded by (10$\bar{1}$) planes, and resolvable into contributions from H-Nb_2O_5 in two twin orientations, with comparable areas of the two twin components. This very extensive twinning in re-formed H-Nb_2O_5 presents some features that need closer examination. Its significance in the present context is, first, that it produces very disordered crystals, and secondly that the twin components seem to be formed with comparable probability. This could indicate that one route for the reoxidation process passes through the formation of structural elements of the forms M- and N-Nb_2O_5 with square 4 × 4 columns. Since the material became structurally ill-defined during reoxidation, the thermogravimetric results reported are confined to reduction runs; the comparability of pseudo-equilibria in the ill defined oxidising direction is doubtful.

End products of the microbalance runs, and strictly comparable materials prepared outside the balance, fell into three groups according to their total composition NbO_x.

$2{\cdot}500 > x > 2{\cdot}495$. On the evidence obtained so far $NbO_{2.495}$ had the unperturbed structure of $NbO_{2.500}$, without detectable local structural rearrangement or Wadsley defects. Whether this implies the accommodation of a fraction $\lesssim 2 \times 10^{-3}$ of vacant oxygen sites is considered further, below.

$2{\cdot}495 > x \geqslant 2{\cdot}480$. In this composition range, different areas within crystal fragments, and different crystal fragments, gave diffraction patterns of H-Nb_2O_5 or of $Nb_{25}O_{62}$ only.

$2{\cdot}480 > x \geqslant 2{\cdot}417$. These materials contained crystals or domains only of $Nb_{25}O_{62}$ and $Nb_{12}O_{29}$ (monoclinic). This was confirmed by examination of a larger specimen, of composition $NbO_{2.460}$, prepared by heating H-Nb_2O_5 in a 20 : 1 CO–CO_2 mixture at 1010 ± 10 °C for 48 h. Reduction under the conditions used in the thermogravimetric runs appears therefore to traverse in turn the three simplest type structures (3). In none of the materials was

$$Nb_{28}O_{70} \longrightarrow Nb_{25}O_{62} \longrightarrow Nb_{12}O_{29} \qquad (3)$$

any evidence obtained for the formation of regular intergrowth structures between these types to give a finer gradation in the composition or defined intermediate phases, although an oxygen-deficient oxide $NbO_{2.483}$ has been identified and assigned the 1 : 1 intergrowth structure $Nb_{53}O_{132}$ by Gruehn and Norin [15] and analogous ternary oxides have been characterized by electron microscopy.

To check whether such intermediate intergrowth phases can be formed, albeit more slowly, at 1000 °C, a separate series of preparations was carried out. $Nb_{25}O_{62}$ was prepared by heating a mixture of $NbO_{2.006}$ and H-Nb_2O_5 in theoretical amounts at 1000 °C in a sealed silica capsule for 120 h. It was characterized by electron diffraction and found to be substantially perfect in structure; lattice images showed regularly spaced (100) fringes (14·5 Å spacing) and doubled (001) fringes (spacing 2 × 10·25 = 20·5 Å), as required by the structure, without Wadsley defects. Two series of preparations were then carried out, by heating oxide mixtures at 1000 °C for 120 h in sealed silica capsules, in the presence of a CO–CO_2 mixture as a self-buffering oxygen transport agent. Compositions were checked, after preparation, by oxidation to Nb_2O_5 on the microbalance, and found to be as specified.

(*a*) Mixtures of $Nb_{25}O_{62}$ with H-Nb_2O_5 in the molar ratios 1 : 2, 1 : 1, and 2 : 1, as required for the known or possible regular intergrowth phases $Nb_{81}O_{202}$ ($NbO_{2.4938}$), $Nb_{53}O_{132}$ ($NbO_{2.4905}$), and $Nb_{39}O_{97}$ ($NbO_{2.4872}$).

(*b*) Mixtures of $Nb_{25}O_{62}$ with $Nb_{12}O_{29}$ (prepared from H-Nb_2O_5 and $NbO_{2.006}$ in a similar manner) were made up to the total compositions $NbO_{2.467}$, $NbO_{2.460}$, $NbO_{2.454}$, $NbO_{2.449}$, and $NbO_{2.438}$ and treated as for series (*a*). Potential intergrowth phases between the structure elements of $Nb_{25}O_{62}$ and $Nb_{12}O_{29}$ include $Nb_{62}O_{153}$ (2 : 1, $NbO_{2.4677}$), $Nb_{37}O_{91}$ (1 : 1, $NbO_{2.4595}$), and $Nb_{49}O_{120}$ (1 : 2, $NbO_{2.4490}$). Analogues of the last two have been identified by electron microscopy in the titanium–niobium ternary oxides.[10c]

In neither set of preparations was any reaction detected at 1000 °C; electron diffraction and microscopy detected no change in the starting materials. Since it is known that

[15] R. Gruehn and R. Norin, *Z. anorg. Chem.*, 1967, **355**, 176.

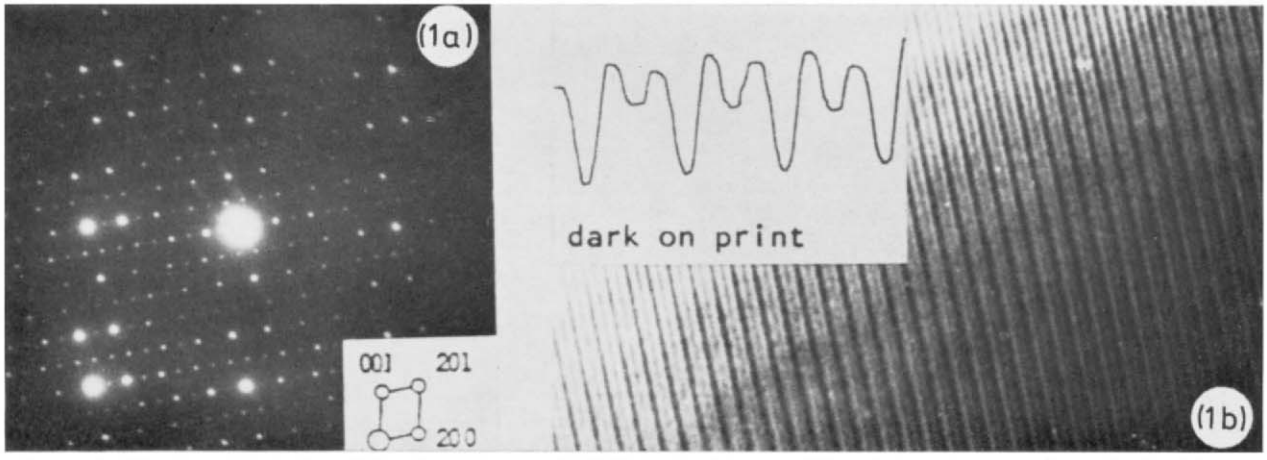

PLATE 1 $Nb_{53}O_{132}$: (a) electron diffraction pattern; (b) (100) lattice fringes. Microphotometer trace shows double fringes corresponding to regular –C–D–C–D– stacking

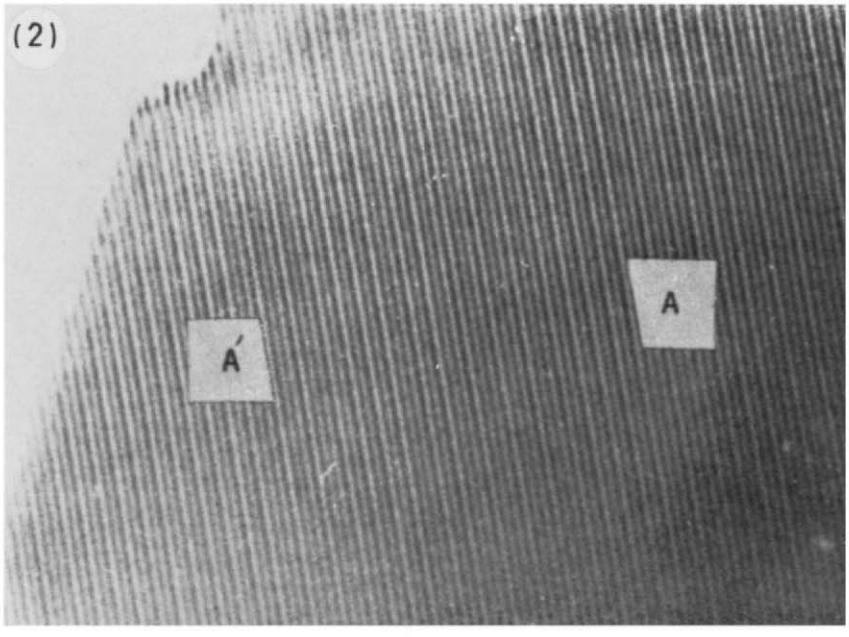

PLATE 2 (100) Lattice fringes from disordered domain in $Nb_{53}O_{132}$

[*To face p.* 2334

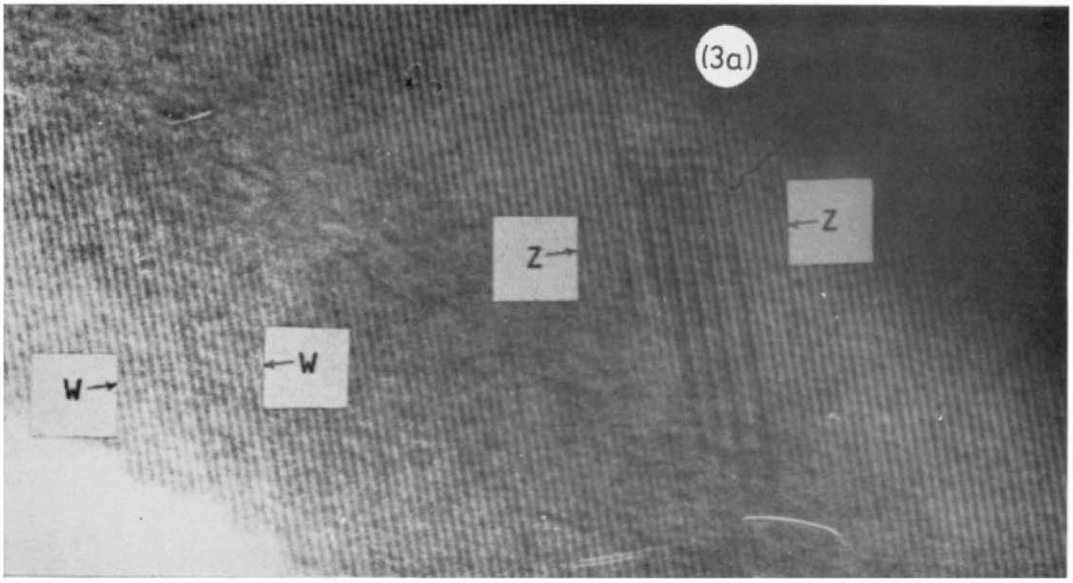

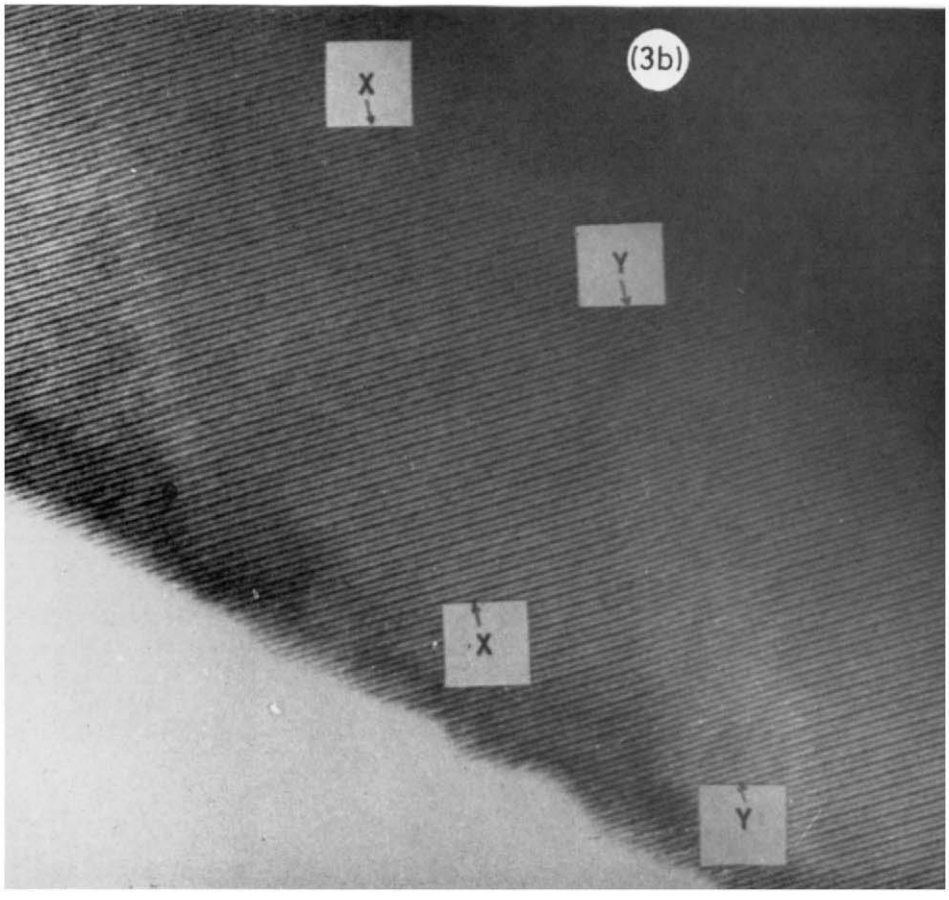

PLATE 3 Disorder in $Nb_{25}O_{62}$: (a) (100) lattice fringes; (b) (001) lattice fringes from the same region

at least one regular intergrowth phase exists, failure to observe reaction could be due to the slowness of diffusion or rearrangement processes. Certain of the preparations were therefore reheated at 1200—1300 °C in an induction furnace, *in vacuo* (10^{-6} Torr). The oxides were not encapsulated for this, and (probably through volatilization of some lower oxide species), their oxygen content (determined) increased during the high-temperature anneal. The products were studied particularly by fringe imaging methods.

Materials with final composition $2{\cdot}4905 > x > 2{\cdot}480$ all contained extensive areas of the 1 : 1 intergrowth phase $Nb_{53}O_{132}$, as shown by the diffraction pattern and the doubled (100) lattice fringe pattern, with alternate spacings of 15 and 17 Å corresponding to the sequence ··C–D–C–D– ··· of stacking rows of $Nb_{25}O_{62}$ and $Nb_{28}O_{70}$ structure (Plate 1; see also Figure 1). In $NbO_{2\cdot481}$

FIGURE 7 Microphotometer trace across A–A′ showing lamella of D–C–C–D–C–C–D– stacking, corresponding to $Nb_{39}O_{97}$

(analysed), formed by oxidation of $NbO_{2\cdot460}$ during annealing, only the $Nb_{53}O_{132}$ and $Nb_{25}O_{62}$ structures were detected; to account for the total composition, it appears that the $Nb_{25}O_{62}$ domains may be oxygen deficient. Defects of stoicheiometry were also observed in the $Nb_{53}O_{132}$ structure. Plate 2 shows (100) lattice fringes from such a crystal, with noticeable variations in spacing, revealed by the microphotometer trace (Figure 7) across the line A–A′ as interpolations of additional 15 Å rows of structure. Each of these represents insertion of a lamella of the stacking sequence –C–C–D–, corresponding to an intermediate oxide $Nb_{39}O_{97}$, of which one strip four unit cells wide (*ca.* 190 Å) is included within the microphotometer trace. These interpolated lamellae probably represent failure to attain true equilibrium, rather than any true stoicheiometric variability in $Nb_{53}O_{132}$.

Materials with final compositions $x < 2{\cdot}480$ also showed defects accommodating a deviation from stoicheiometry. Plate 3 shows both (100) and (001) lattice fringes from a domain of $Nb_{25}O_{62}$ in an annealed sample. A single narrow fringe (13 Å; denoted by K) is inserted (Figure 8) in the set of 15 Å (100) fringes in the strip W–W′; between Z–Z there is a regular succession of the stacking sequence ···C–K–C–K–C–K– ··· forming a lamella of a regular intergrowth. In the (001) fringes, a microphotometer trace across the line X–X shows the doubled 20·5 Å fringe

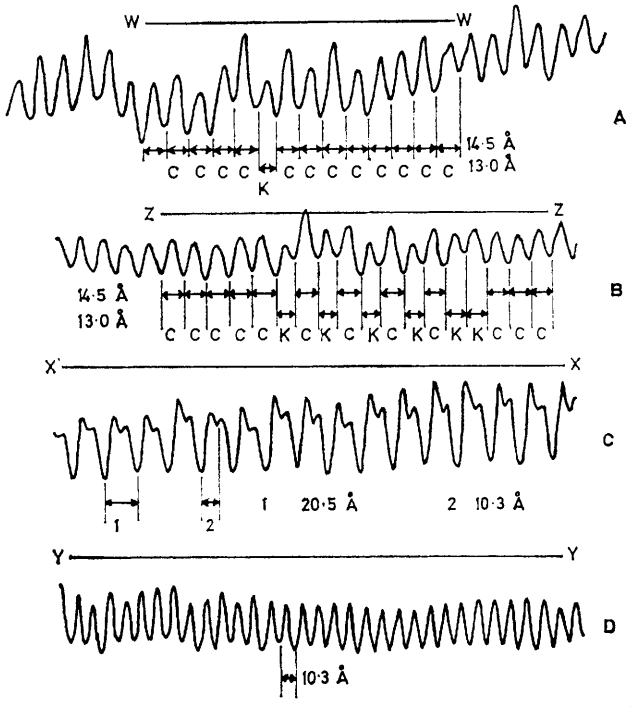

FIGURE 8 Microphotometer traces across marked sections of Plate 3. A, (100) Fringes across W–W′ [Plate 3(a)] showing one narrow K fringe implying a strip with (3 × 3) columns; B, (100) fringes across Z–Z′: four unit cells of C–K–C–K intergrowth and two adjacent K fringes equivalent to a lamella of $Nb_{22}O_{54}$; C, (001) fringes across X–X′ [Plate 3(b)] showing doubled fringes (2 × 10·25 Å = 20·5 Å) of unequal intensity in $Nb_{25}O_{62}$; D, (001) fringes across Y–Y′ showing equivalent fringes of *ca.* 10·3 Å spacing in the intergrowth lamella

system, with contrast maxima of unequal intensity, proper to $Nb_{25}O_{62}$. Allpress has associated this intensity distribution with the unequal density of scattering atoms along alternate (002) planes. Across the line Y–Y, through the strip of intergrowth, fringes of equal intensity are spaced

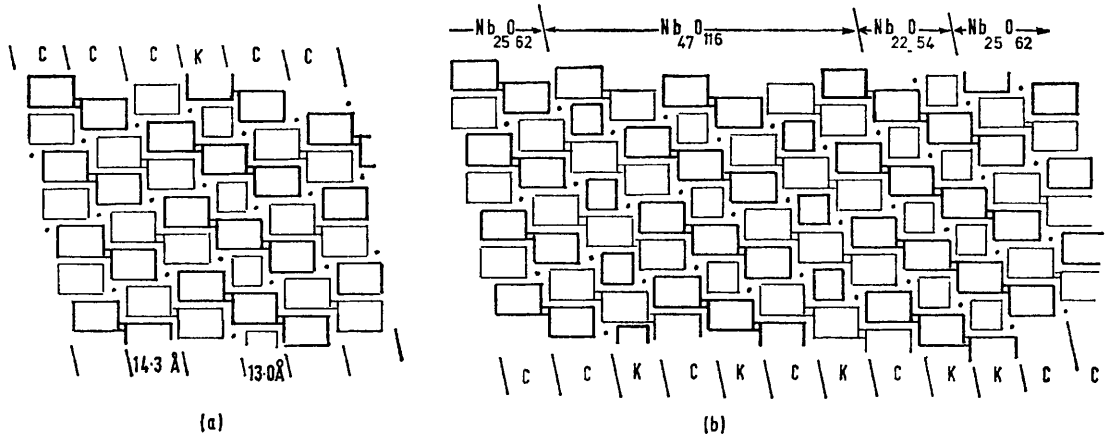

FIGURE 9 (a) The single intergrown strip of $Nb_{22}O_{54}$ structure shown by Figure 8, B; (b) the structure revealed by Figure 8, C and 8, D, with an intergrowth of $Nb_{47}O_{116}$

at 10·25 Å. Across the lamella of intergrowth, the (001) fringes of $Nb_{25}O_{62}$ are displaced by half a fringe. These characteristics serve to identify the K row as an element of the $Nb_{22}O_{54}$ structure (Figure 9), and the intergrowth as a strip of $Nb_{47}O_{116}$. Significant oxygen deficiency in $Nb_{25}O_{62}$ is therefore accommodated by building in coherently compatible strips of a lower oxide, which tend to generate a regular 1 : 1 intergrowth. Under conditions favourable to recrystallization, as in the preparative method of Gruehn and Norin, this is the equilibrium product. Its formation from $Nb_{25}O_{62}$ structure and $Nb_{12}O_{29}$ structure (1000 °C components) requires a structural rearrangement, as well as an ordering process.

DISCUSSION

The Reduction Equilibria.—It is clear that, notwithstanding the apparently bivariant form of the $(T,x)_p$ and $(p,x)_T$ curves, the solid phase in each of the composition ranges $NbO_{2.500}$—$NbO_{2.480}$ and $NbO_{2.480}$—$NbO_{2.417}$ was structurally inhomogeneous, with two stoicheiometrically defined structures coexisting. At the composition $NbO_{2.480}$ it was essentially monostructural, even though this composition was marked by no step or singularity in the isobars. There is some evidence that, at around this composition, all three structures may be present simultaneously, in different domains. The system does not behave as a classical Gibbs phase assembly. The 'equilibrium' curves may better be regarded as segments of two overlapping hysteresis loops, as found for systems with a multiplicity of intermediate phases related to crystallographic shear (*e.g.*, the TiO_{2-x} system).[16] The several structures do not have uniquely specified intensive thermodynamic properties; they are coherently intergrown and the solid phase might be described, in Ubbelohde's terms, as an assembly of hybrid crystals.

In view of the difficulty of specifying the behaviour in classical thermodynamic terms, the several species have been consistently defined in terms of their observed *structures*, not as *phases*. Further, although each crystallographically defined structure specifies the Nb : O *site ratio*, the available evidence does not necessarily imply an equally definite *composition*. The role of defects in these oxides has not been finally clarified. In the materials treated at 1200—1300 °C, which approach inner equilibrium, it is evident that deviations from ideal composition in excess of some limited range are accommodated by interpolation of rows of 'wrong' columns, with a different but defined composition. Such interpolated rows are planar defects of the Wadsley type. It is not certain that the smallest detectable deviations from ideal composition take this form. Reference has been made to the lack of evidence for planar defects in the H-Nb_2O_5 structure, at compositions down at least to $NbO_{2.495}$. There is other evidence favouring the occurrence of point defects (probably oxygen vacancies) in 'block' structures. $Nb_{25}O_{62}$ is reported as having a stoicheiometric range, with the upper existence limit oxygen-deficient, at $NbO_{2.478}$; the intergrowth structures $Nb_{53}O_{132}$ and $Nb_{47}O_{116}$ have been found for materials with the reproducible compositions $NbO_{2.483}$ and $NbO_{2.463}$ respectively, and Gruehn has pointed out that these compositions correspond to intergrowths of the most oxygen deficient component structures.[17] In specifically searching for planar defects to account for stoicheiometric variability, Allpress has found that the $WNb_{12}O_{33}$ structure appears to be homogeneous, at the level of electron microscopic examination, over the range $WO_3,6Nb_2O_5$ to $WO_3,8Nb_2O_5$ ($\equiv M_{13}O_{32.8}$).[18] Finally, *X*-ray diffraction evidence indicates that $GeO_2,9Nb_2O_5$ is isostructural with PNb_9O_{25}, a $(3 \times 3)_1$ block structure;[19] if all cation sites are filled, this would imply the composition $M_{10}O_{24.7}$. The evidence for oxygen-deficient structures is fairly strong, but more thorough investigation is needed.

The Role of Kinetics and Mechanism of Reaction.—The high-temperature experiments leave little doubt that intergrowth structures, particularly $Nb_{53}O_{132}$ and $Nb_{47}O_{116}$, are stable species, and that the $Nb_{12}O_{29}$ and $Nb_{25}O_{62}$ structures do not coexist in true equilibrium. The equilibrium sequence of compounds appears to be $Nb_{28}O_{70} \longrightarrow Nb_{53}O_{132} \longrightarrow Nb_{25}O_{62} \longrightarrow Nb_{47}O_{116} \longrightarrow Nb_{22}O_{54} \longrightarrow Nb_{12}O_{29}$, with a structural rearrangement, to create (3×3) columns, in the reduction of $Nb_{25}O_{62}$. It follows that the course of reactions is determined by two kinetically distinct types of process: (i) one relatively easy and rapid at 1000 °C, that virtually cuts up the $(5 \times 3)_\infty$ ribbons of H-Nb_2O_5 into (4×3) columns, and then links (4×3) columns into ribbons, and (ii) a process of higher activation energy, extremely slow at 1000 °C but usefully rapid above 1200 °C, that brings columns of different sizes into an equilibrium ordering, with some rearrangement of column cross sections if required. This step requires a complete reshuffle of the interfaces between columns throughout the crystal at each stage. Although the atomic displacements at each step are small (in general a shift from the original site to an adjacent interstitial site) the activation energy is probably similar to that of a unit diffusion step, the free-energy gain is small, and the rate is probably determined by the slower (cation) self-diffusion rate.

The lower-temperature processes take place surprisingly rapidly and can therefore involve no gross reconstruction. They proceed so as to preserve coherence between parent and product structures and operate on successive units of the structure so as to build up progressively thickening slabs of the product. The electron microscopy suggests that reaction may be nucleated at random and that the lamella of transformed structure grows into the crystal along bounding coherence planes, initially as an isolated Wadsley defect.

[16] R. R. Merritt and B. G. Hyde, personal communication; in course of publication.
[17] R. Gruehn, Proceedings 5th Materials Research Symposium, N.B.S. Special Publication 364, 1972, p.63.
[18] J. G. Allpress and R. S. Roth, *J. Solid State Chem.*, 1971, **3**, 209.
[19] E. M. Levin, *J. Res. Nat. Bur. Stand.*, 1966, **70**, *A*, 5.

This parallels behaviour found in simpler oxide systems. It has been observed [20] that when rutile suffers reduction in the electron beam, isolated crystallographic shear planes grow inwards from the surface, across the crystal, terminating in a dislocation if they do not traverse the entire width. Whilst the mechanism of formation of crystallographic shear planes is not settled, many of the facts can be interpreted by the model advanced by Anderson and Hyde.[21] Abstraction of oxygen from surface sites leads to local collapse and formation of a disc of crystallographic shear structure, bounded by a dislocation loop. This climbs through the crystal, extending the area of the crystallographic shear plane. As originally advanced, it was suggested that oxygen atoms were lost at random, the vacancies then draining into, and being eliminated by, the climbing dislocation. It is more probable that the strain field locally raises the chemical potential of oxygen, so making the dislocation the preferred site for reduction.

The relevance of these considerations is that the concept of crystallographic shear can be applied to the reduction of H-Nb_2O_5. Examination of the structural relations between the three basic types of structure, $Nb_{28}O_{70}$, $Nb_{25}O_{62}$, and $Nb_{12}O_{29}$, shows that each of these can be converted into the next by a crystallographic shear. Denoting the displacement by a short unit vector of the ReO_3-type sub-cell (indicated by subscript R) and the operant plane by its Miller indices in the matrix structure (H-Nb_2O_5 or $Nb_{25}O_{62}$ respectively), we readily see that the crystallographic shear operations $a_R[00\bar{1}]_R/(001)$(H-Nb_2O_5) and $a_R[00\bar{1}]/(001)$-($Nb_{25}O_{62}$) would generate coherent rows of $Nb_{25}O_{62}$ and of $Nb_{12}O_{29}$ structure respectively. Whether this structural relationship provides a valid insight into the transformation process is not so clear. Whereas crystallographic shear in the simple binary oxide structures (rutile, WO_3, MoO_3) eliminates a sheet of anion sites only, it implies in the block structures the elimination of both anion and cationic sites, in different proportions. Propagation of a crystallographic shear collapse into a crystal would therefore involve a flow of both oxygen and metal atoms along the diffusion path provided by the bounding dislocation. Other reaction mechanisms (*e.g.*, of the Wadsley–Andersson type [22]) would involve just those lateral diffusion and reshuffling steps that appear from the difference in the reaction route at 1000 °C and 1200—1300 °C, to be kinetically inhibited.

We thank the Atomic Energy Research Establishment for support and the Royal Society for provision of the goniometer stage for the JEM 6A microscope. We are indebted to JEOL (UK) Ltd. for facilities for high electron microscopy.

[2/1140 *Received*, 19*th May*, 1972]

[20] J. S. Anderson and R. J. D. Tilley, *J. Solid State Chem.*, 1970, **2**, 472.

[21] J. S. Anderson and B. G. Hyde, *J. Phys. Chem. Solids*, 1967, **28**, 1393.

[22] S. Andersson and A. D. Wadsley, *Nature*, 1966, **211**, 581.